Numerical Analysis of Electric Field in Three-Electrode Corona System Containing Ionized and Non-Ionized Areas

R. Barciauskas[1], P. Marciulionis[1], S. Zebrauskas[1]
[1]*Department of Electric Power Systems, Kaunas University of Technology, Studentu St. 48–236a, LT-51367 Kaunas, Lithuania*
ricka.bar@gmail.com

***Abstract*—In many corona field applications, three-electrode and multi-electrode systems with different electrode potentials are being used. Procedure and results of numerical analysis of direct current corona field in three-electrode corona system consisting of ionizing wire placed between two parallel non-ionizing electrodes is presented in this paper. Algorithm of analysis consists of two stages. Stage 1 comprises an electrostatic approach of field analysis without space charges. Result of this stage is an equation of separatrix dividing the field into 2 areas: an area of electric flux between the corona wire and one of plane electrodes, and an area occupied by the flux between the plane electrodes. Stage 2 involves numerical analysis of the field in both areas. Numerical model is based on the assumption that the space charge of corona field doesn't change the position and shape of separatrix. Results of modelling are validated experimentally. Proposed method of analysis allows predicting the behaviour of multi-electrode corona system using finite computer resource.**

***Index Terms*—Corona, finite difference methods, numerical analysis, space charge.**

I. INTRODUCTION

Large number of two-electrode corona discharge systems used in many applications consists of ionizing electrode (wire, needle, etc.) and non-ionizing electrode. Corona fields of these systems usually are assumed as plane-parallel or axially symmetric ones. Functional possibilities of corona devices may be enhanced by use of multi-electrode system. Unfortunately, more complicated models are needed for analysis of the field in multi-electrode systems. Models of an electrostatic field in roll-type separator discussed in [1] are published more than 20 years ago. Given models of three-electrode system with ionized and non-ionized field areas demonstrate the complexity of the problem. Boundary element method is employed for analysis of the electrostatic field distribution in the roll-type separator [2], consisting of wire-type corona electrode, ellipse-profile non-ionizing electrode and grounded cylindrical one. Numerical model is proposed in [3] for solving the differential equations that describe the combined corona-electrostatic electric fields. The aim of the research is to overcome the limitation of the previous works related to the fact that the employed programs were not capable to simulate the distortion of the electric field due to the presence of the space charge. Publication [4] is the further development of ideas given in [3]. Mathematical model of the field generated between the ionizing wire, cylindrical conducting tube and the grounded collecting plate is based on a conformal mapping that converts the actual boundary-free field area into a rectangular domain with well-defined boundary conditions. The finite-difference method is used for solving the differential equations describing the field in this domain.

The field of corona triode consisting of parallel ionizing wires, a grounded collecting plane electrode and parallel grid rods between them is analysed in [5] using the finite-element and boundary element methods combined with the method of characteristics. The distribution of field strength, space-charge density and current density, also the discharge current can be controlled by changing the grid voltage and configuration of electrode system. The total corona current is the sum of the current directed from ionizing wires to collecting plate and the current between wires and the grid.

An analytical model is developed to calculate the ion number concentration and mean charge per particle in the charging zone of the particle charger consisting of two concentric metal cylinders and a corona-wire placed along the axis of the cylinders [6]. Outer cylinder is connected to the ground. The ion driving voltage applied on the inner cylinder forces the ions through the perforated screen openings on the inner cylinder to the charging zone. Analysis of the field in this triode charger is performed by use the assumption of neglected space charge due to the ions. Electric fluxes between the emitting and collecting electrodes as well as between the emitting and control electrodes in [5] are related with the ionized areas of the field.

Our concept is to develop the principle of discharge current from the emitting electrode control without a current related to control electrode. Electrostatic field in the system "corona wire between two parallel plane electrodes with different potentials" is studied in [7]. Analysis of the field is based on the use of the superposition of complex potentials in wire-to-plane electrode system and in the system of parallel plane electrodes. Modes of the field-line behaviour are determined depending upon the values of electrode

Manuscript received October 25, 2013; accepted January 17, 2014.

potentials and the system configuration. Equation of separatrix, dividing the field of the system into two areas: the area occupied by electric flux directed from the corona wire to the one of plane electrodes and the area of the flux between plane electrodes was constructed in [8]. Parameters of corona field electrometer [9] are determined as a result of field computation by use the Deutsch´s assumption: vector of the corona field strength differs in magnitude from the strength of Laplacean field, but their directions coincide [10], [11].

The subject of this work is to validate an analytical-numerical model for computing the two-dimension field of three-electrode corona device comprising of ionized and non-ionized areas. Our investigation consists of two steps. Analysis of electrostatic field in three electrode system without the space charge shown in Fig. 1 is being performed in the first stage. Result of the analysis is the equation of separatrix dividing the field into areas occupied by different electric fluxes. The second stage comprises of the numerical modelling of the corona field under the assumption that the space charge does not influences the shape and position of separatrix.

II. MATHEMATICAL MODEL

A. Step 1. Electrostatic Approach

Analysis of two-dimensional electrostatic field in three-electrode system without space charge shown in Fig. 1 was performed in [7]. Complex potential

$$w(x,y) = u(x,y) + \mathrm{j}v(x,y), \tag{1}$$

was determined by superposition of the homogeneous field and the field generated by a set of parallel charged wires. Potential function u and stream function v were obtained as:

$$u(x,y) = k_2 \cdot \ln S_0 + u_1 + E_0 \cdot (h_1 - x), \tag{2}$$

$$v(x,y) = k_2 \cdot ¤ - E_0 \cdot y, \tag{3}$$

where:

$$E_0 = (u_3 - u_1)/(h_1 + h_2), \tag{4}$$

$$k_2 = (u_1 + E_0 \cdot h_1)/k_{\mathrm{geom}}, \tag{5}$$

$$k_{\mathrm{geom}} = 0{,}5 \cdot \ln \frac{\sin^2(k_h h_1) \cdot \sin^2\left[k_h (r_0 + 2h_2)\right]}{\sin^2(k_h r_0) \cdot \sin^2\left[k_h (h_1 + 2h_2)\right]}, \tag{6}$$

$$k_h = ®/2(h_1 + h_2), \tag{7}$$

$$S_0 = \sqrt{\frac{\sin^2(k_h h_1) + \mathrm{sh}^2(k_h y)}{\sin^2\left[k_h (x + 2h_2)\right] + \mathrm{sh}^2(k_h y)}}, \tag{8}$$

$$¤ = \arctan\left[\cot(k_h x) \cdot \tanh(k_h y)\right] - \arctan\left[\cot\left(k_h (x + 2h_2)\right) \cdot \tanh(k_h y)\right], \tag{9}$$

Electric flux related to electrodes u_2 and u_3 in Fig. 1 is equal to 0 if there is a point on the axis x between these electrodes with the zero value of the field strength [8]. Separatrix is a line denoting the geometric place of points where the imaginary part of complex potential $v(x, y)$ is equal to 0. An equation of separatrix dividing the field into two areas: an area occupied by an electric flux related to electrodes u_1 and u_2 and an area with the flux between electrodes u_1 and u_3 is derived in [9]. The field in the first area is strongly inhomogeneous, and the field between electrodes u_1 and u_3 is quasi-homogeneous. The view of equipotential and field lines for the electrometric mode of field [7] is shown in Fig. 2. It corresponds to the following values of parameters: h_1 = 10.0 mm, h_2 = 40.0 mm, r_0 = 0.025 mm, u_1 = –10000 V, u_2 = 0, u_3 = –5000 V. Distances in the field view are given in milimetres. Dashes correspond to equipotentials and field lines are marked by continuous ones.

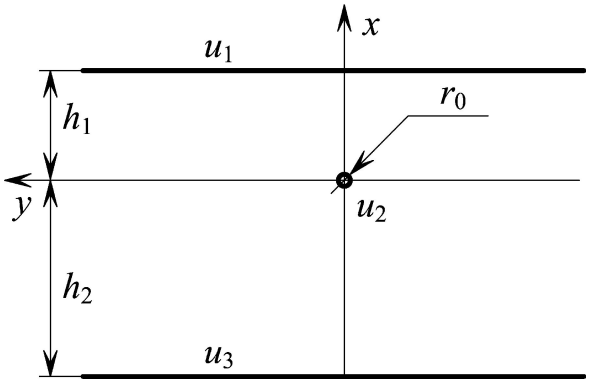

Fig. 1. Configuration of the electrode system under study.

Equation of separatrix is the following [12]

$$k_2 \cdot ¤ - E_0 \cdot y = 0. \tag{10}$$

Coordinates of separatrix points are given in Table I for the step Δx = 1.0 mm.

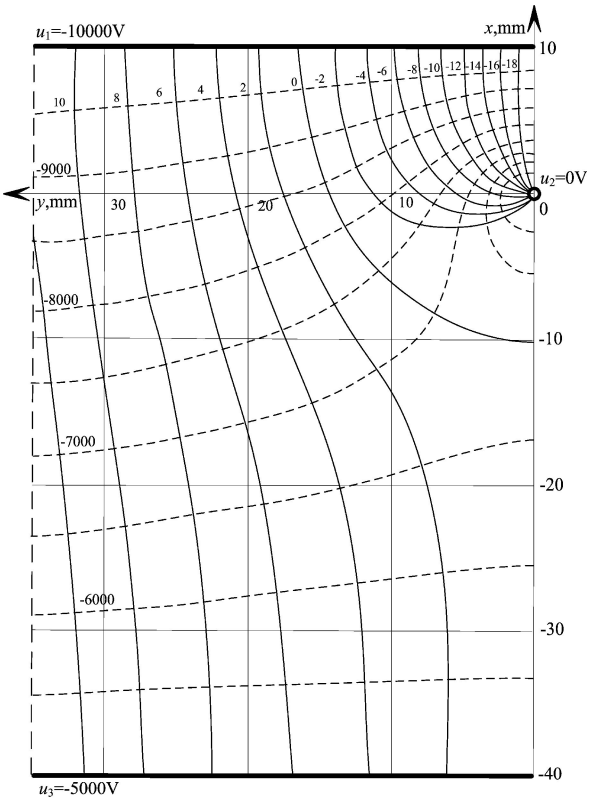

Fig. 2. Equipotential and field lines of electrostatic field.

TABLE I. COORDINATES OF SEPARATRIX POINTS.

x, mm	*y*, mm	*x*, mm	*y*, mm
10.0	16.4	–10.3	0
9.0	16.4	–9.0	3.2
8.0	16.3	–8.0	7.8
7.0	16.3	–7.0	9.5
6.0	16.2	–6.0	10.0
5.0	16.0	–5.0	11.1
4.0	15.7	–4.0	12.6
3.0	15.4	–3.0	13.2
2.0	15.1	–2.0	14.1
1.0	14.9	–1.0	14.8
0	14.8	0	14.8

B. Step 2. Corona field

We use the finite difference method for the 2D numerical modelling of the field. Rectangular mesh in Cartesian system of coordinates is suitable for the analysis in the non-ionized part of the field. Polar system of coordinates must be used for analysis of corona field. The fragment of the field is shown in Fig. 3.

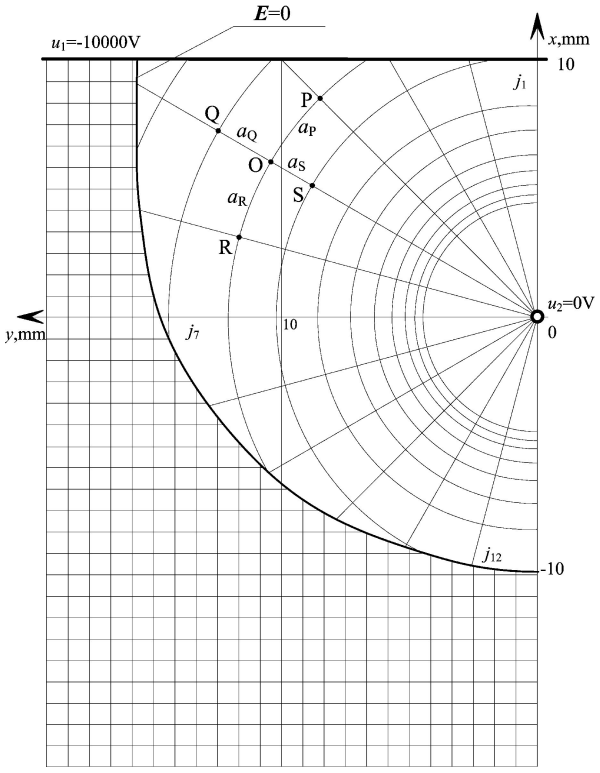

Fig. 3. Fragment of the field with rectangular mesh to the left of the separatrix and with polar mesh to the right of it.

Numerical analysis of corona field is based on the assumption that space charges don't change the coordinates of separatrix points determined by an electrostatic approach. Corona field is governed by the system of equations [13]:

$$\begin{cases} \mathrm{div}\mathbf{E} = \rho/\varepsilon_0, \\ \mathbf{E} = -\mathrm{grad}u, \\ \mathrm{div}\mathbf{J} = 0, \\ \mathbf{J} = \rho k\mathbf{E}, \end{cases} \tag{11}$$

where $\boldsymbol{E}$ is electric field strength, $\boldsymbol{J}$ is current density, ρ is space charge density, u is potential, ε is permittivity, and k is ion mobility. We use [9] the system (11) reduced to the Poisson's and charge conservation equations as in [2], [4]:

$$\mathrm{div}\,\mathrm{grad}u = -\rho/\varepsilon, \tag{12}$$

$$\mathrm{grad}\rho \cdot \mathrm{grad}u = \rho^2/\varepsilon. \tag{13}$$

Laplace's equation describes the field in the non-ionized area

$$\mathrm{div}\,\mathrm{grad}u = 0. \tag{14}$$

Finite difference approximation of this equation for the regular mesh represents the averaging of potential values at four surrounding points

$$u(i,j) = 0,25\big[u(i+1,j) + u(i-1,j) + u(i,j+1) + u(i,j-1)\big]. \tag{15}$$

Irregular rectangular mesh is characterized by the distances a_S, a_Q, a_P and a_R from the central node O to surrounding nodes P, Q, R and S (similar as in Fig. 3). Laplace's equation in finite differences is of the following form

$$\frac{a_S u(x_0+a_Q, y_0) - (a_Q+a_S)u(x_0,y_0) + a_Q u(x_0-a_S, y_0)}{0,5a_Q a_S(a_Q+a_S)} + \frac{a_P u(x_0, y_0+a_R) - (a_P+a_R)u(x_0,y_0) + a_R u(x_0, y_0-a_P)}{0,5a_P a_R(a_P+a_R)} = 0. \tag{16}$$

Finite difference approximation of Poisson's equation in polar irregular mesh is defined as

$$\frac{2u_P}{a_P^2+a_P a_R} + \frac{2u_R}{a_R^2+a_P a_R} + \frac{2u_Q}{a_Q^2+a_Q a_S} + \frac{2u_S}{a_S^2+a_Q a_S} + \frac{u_Q a_S}{r_1\left(a_Q^2+a_Q a_S\right)} - \frac{u_S a_Q}{r_1\left(a_S^2+a_Q a_S\right)} - u_O\left(\frac{2}{a_Q a_S} + \frac{2}{a_R a_P} + \frac{a_S^2-a_Q^2}{r_1\left(a_Q a_S^2 + a_S a_Q^2\right)}\right) = -\frac{\rho_O}{\varepsilon}. \tag{17}$$

Meanings of letters a_S, a_Q, a_P and a_R are the same as in (16) – see Fig. 3. Central angle between the neighbour radii of the regular polar mesh can be written as

$$\alpha_0 = 2\pi/m, \tag{18}$$

where $m + 1$ is the quantity of radial lines, for the mesh shown in Fig. 3, $m = 12$. Radial coordinate r is defined as follows

$$r = r_0 \beta^{i-1}, \tag{19}$$

where $\beta = 1+\alpha_0$, i is the number of the node on the radial line. Poisson's equation for the regular polar grid is of the following form

$$u_O = 0,25\big[u_P + u_R + (1+0,5\alpha_0)u_Q + (1-0,5\alpha_0)u_S\big] + \rho_o/\varepsilon. \tag{20}$$

Finite difference approximation of the charge conservation equation in the polar coordinate system contains derivatives with respect to r and φ [14]

$$\frac{\partial °}{\partial r}\cdot\frac{\partial u}{\partial r}+\frac{1}{r}\frac{\partial °}{\partial ¤}\cdot\frac{1}{r}\frac{\partial u}{\partial ¤}=\frac{°^2}{£}. \quad (21)$$

Finite-difference approximations of these derivatives are the following:

$$\frac{\partial u}{\partial r}=-\frac{u_S a_Q}{a_S\left(a_Q+a_S\right)}+\frac{u_Q a_S}{a_Q\left(a_Q+a_S\right)}+\frac{u_O\left(a_Q-a_S\right)}{a_Q a_S}, \quad (22)$$

$$\frac{\partial u}{r\partial ¤}=\frac{u_R\ a_P/a_R-u_P\ a_R/a_P}{\left(a_P+a_R\right)}+\frac{u_O\left(a_P-a_R\right)}{a_P a_R}. \quad (23)$$

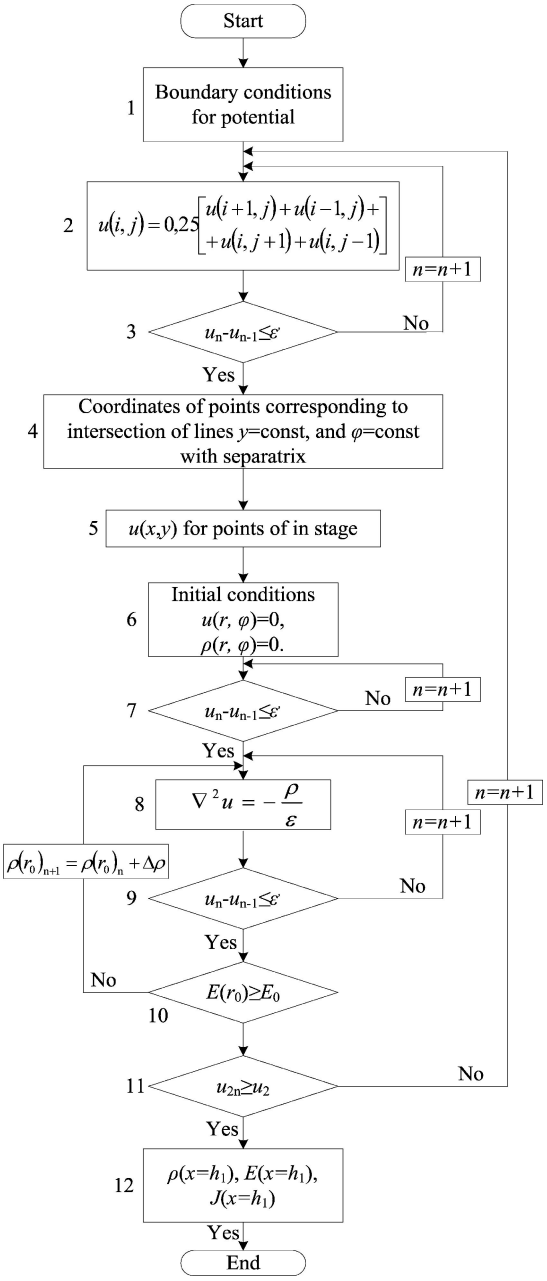

Fig. 4. Computational scheme for the numerical analysis of the field.

Corresponding formulas for charge density derivatives are similar:

$$\frac{\partial °}{\partial r}=\frac{°_Q a_S}{a_Q\left(a_Q+a_S\right)}-\frac{°_S a_Q}{a_S\left(a_Q+a_S\right)}+\frac{°_O\left(a_Q-a_S\right)}{a_Q a_S}, \quad (24)$$

$$\frac{\partial °}{r\partial ¤}=\frac{°_R\ a_P/a_R-°_P\ a_R/a_P}{\left(a_P+a_R\right)}-\frac{°_O\left(a_P-a_R\right)}{a_P a_R}. \quad (25)$$

Dirichlet boundary conditions for electrode potentials are the constant values of u_1, u_2 and u_3 (Fig. 2). Boundary condition for the node potentials on the symmetry axis $y = 0$ is an equality $u_P = u_R$ for each node of that line. Condition for the nodes of the free boundary line $y = 0{,}5\ l$, (l is the length of the plane electrodes), is the following

$$u(i,j)=(1/h)\left[u(i-1,j)(h-1)+u(i-2,j)\right], \quad (26)$$

where h is the length of the step. These conditions are being determined in the 1 stage of the algorithm given in Fig. 4.

Stages 2 and 3 comprise the solution of Laplace′s equation in Cartesian coordinates for all domain of the field, n is the number of iteration, ε' is accuracy. Coordinates of separatrix points are being computed in the Stage 4, and their potentials are determined in the Stage 5. Boundary conditions for the points of separatrix are described in details in [15]. Initial conditions for the Laplacean field in polar coordinates are established in Stage 6, Stages 7 and 8 are the solution of Poisson equation. We use the Kaptzov′s assumption [12] to determine boundary conditions on the surface of corona wire: electric field strength on the surface $E_{(ro)}$ is proportional to the voltage below the corona onset U_0, and stays constant and equal to the initial field strength value E_0 determined from Peek′s formula for $U \ge U_0$ [16]. To fulfil this condition the space charge density on the surface of corona wire $\rho(r_0)$ is changed iteratively (Stage 10). Procedure closes if the potential of emitting wire exceeds the given value (Stage 10). Current density on the surface of plane electrode 1 is determined at the end

$$J\left(x=h_1\right)=°\left(x=h_1\right)\cdot k\cdot E\left(x=h_1\right). \quad (27)$$

III. Results Of Numerical Modelling

Input quantities for numerical modelling of the field are the same as in electrostatic approach [17]: h_1 = 10.0 mm, h_2 = 40.0 mm, r_0 = 0.025 mm, distance from the edge of plane electrodes to the x axis l = 200 mm, electrode potentials u_1 = –10000 V, u_2 = 0, u_3 = –5000 V. Mobility of negative ions k_- = $2.2\cdot10^{-4}$ m^2/(V·s) = const.

Total number of nodes in the Laplacean field grid is 10104 (for the step $\Delta x = \Delta y$ = 1.0 mm), the number of nodes in corona field grid is 671 (for central angle of polar grid $\varphi_0 = \pi/12$). The number of nodes in the Laplacean field grid may be essentially reduced by minifying the length l.

Distribution of the field strength $E(x)$ on the axis of symmetry is presented in Fig. 5. Interval of coordinate $-40 \le x \le -10$ mm corresponds to the field without space charge. Field strength equals to 0 in the separatrix point x = –10 mm. Interval of x to the right of this point gives the values of corona field strength. Maximum value of the strength

equal to the 211.3 kV/cm is reached on the surface of the wire.

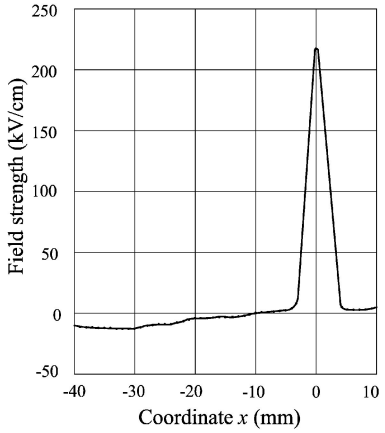

Fig. 5. Distribution of field strength $E(x)$ on the axis of symmetry.

Distribution of potential on the axis of symmetry is given in Fig. 6. Interval $-40 \le x \le -10$ mm corresponds to the potential of Laplacean field, and the values of x in the rest interval $-10 \le x \le 10$ mm are arguments of potential as a solution of corona field equations. Potentials of all wire surface points are equal to 0.

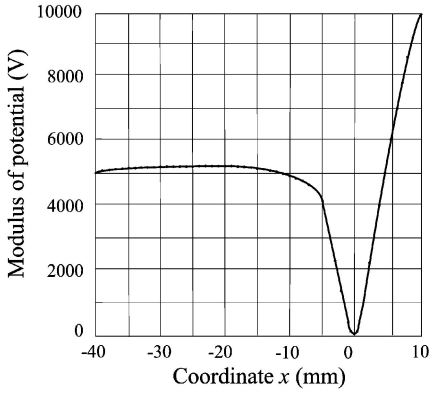

Fig. 6. Distribution of potential $u(x)$ on the axis of symmetry.

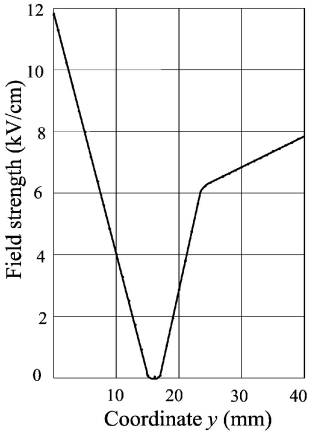

Fig. 7. Field strength $E(y)$ on the surface of plane electrode u_1 (x = 10.0 mm).

Dependence of the field strength upon the values of coordinate y on the surface of plane electrode u_1 (x = 10.0 mm = const) is shown in Fig. 7. Field strength is equal to 0 in a point y = 16.4 mm, i.e. in the boundary point of separatrix. Field strength values in the points to the left of mentioned point correspond to the solutions of electrostatic field without space charges, and the values of field strength in the points to the right of mentioned one are the solutions of corona field equations.

Figure 8 presents a graph of space charge density $\rho(y)$ on the surface of plane electrode u_1. Space charge density $\rho(y)$ equals to 0 in all points $y \ge 16.4$ mm.

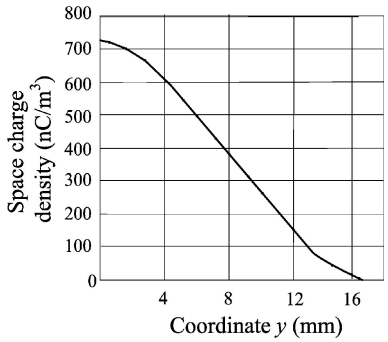

Fig. 8. Space charge density $\rho(y)$ on the surface of plain electrode 1.

Figure 9 shows the schematic diagram of experimental set-up. Potentials of all electrodes are shifted by the constant u_1 = 10000 V in comparison with those used in numerical modelling: u_1 = 0, u_2 = 10000 V and u_3 = 5000 V.

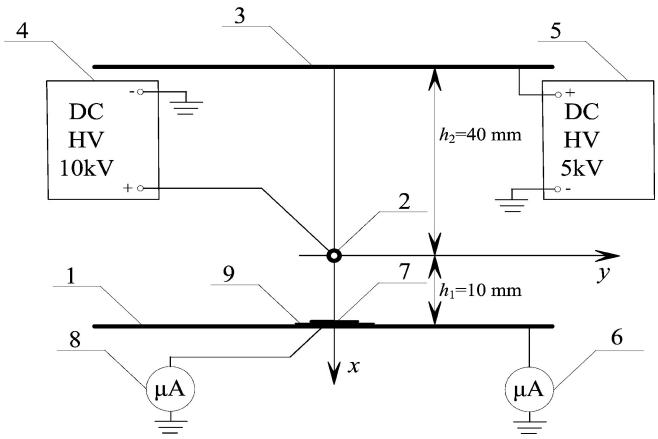

Fig. 9. Schematic diagram of experimental set-up.

Adjustable direct current high voltage power supply units 4 and 5 are used to maintain given values of electrode potentials. Unit 4 is connected to the wire 2, and the one 5 is connected to the plane electrode 3. Plane electrode 1 is grounded via microammeter 6 destined for measurement of the total electrode current. Narrow conductive strip 7 is attached to the plane electrode 1 and insulated by means of dielectric layer 9. Microammeter 8 connected to the strip 7 is used for measurement of the current density. Position of the strip 7 in respect of the origin of coordinate system can be adjusted by means of the micrometric screw (not shown in Fig. 9). Rotation of the screw causes the movement of the plane electrode 1 with the attached strip 7 in direction of coordinate axis y.

Corona current density distribution on the surface of plane electrode 1 experimental data are given in Fig. 10 (dots). Computer modelling data are also presented here (asterisks). Current density is determined from (27) using ρ and E values given in Fig. 7 and Fig. 8.The value of coordinate y = 16.4 mm corresponds to the boundary point of separatrix on the surface of the plane electrode 1. Measured value of this coordinate is 17.2 mm. Discrepancy between the measured and theoretical values of coordinate y determining the

position of boundary point of separatrix is 4.6 %.

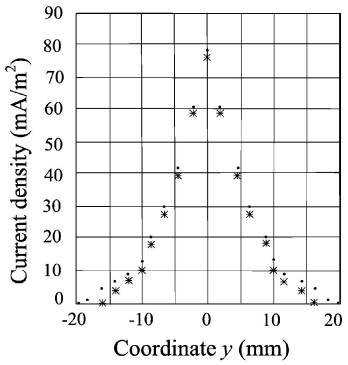

Fig. 10. Distribution of current density on the surface of plane electrode 1.

Total current of plane electrode 1 is determined by numerical integration of current density

$$I = 2\int_0^{y_s} J(y)\mathrm{d}y, \tag{28}$$

where y_s = 16.4 mm. Measured value of corona current determined from (28) is 420 μA/m, corresponding computed value of corona current is 441 μA/m. Discrepancy of these values is 4.8 %. Differences between the measured and computed values of total corona current alike between the values of boundary point coordinates on the surface of plane electrode 1 may be caused by the main assumption of computer modelling, by the used constant value of ion mobility and by the finite accuracy of measuring devices.

IV. CONCLUSIONS

Numerical method for analysis of electric field in three-electrode system "corona wire between two plane electrodes with different potentials" consisting of ionized and non-ionized areas is proposed. The method involves two stages. Laplacean field of the electrode system is being analysed in the first stage where an equation of separatrix dividing the field into areas with electric fluxes related and not related to the corona wire is derived. In the second stage, finite difference method is used for numerical solution of Laplace′s and corona field equations. Equality of Laplacean field and corona field potentials in the nodes of separatrix is the boundary condition for this line. Boundary condition for nodes of separatrix is based on the main assumption of the paper that the space charge of corona field doesn′t change the position and shape of separatrix determined in the stage of electrostatic approach. Validation of numerical modelling data is performed by measuring the corona field density on the surface of plane electrode in the ionized area. Difference between measured and computed values of coordinate that defines position of separatrix boundary point is 4.6 %. Values of measured and computed corona current in the ionized area differs by 4.8 %. Proposed model is accurate enough for computer simulation to be able to solve effectively problems of corona field in multielectrode systems of practical interest. This method is suitable for analysis of corona field in other multielectrode systems, such as "a set of corona wires between parallel plane electrodes", "corona wire or a set of wires between cylindrical and plane electrodes", etc. Moreover, from practical point of view, the study of the Laplacean field distribution in the first stage can guide the designer to predict the behaviour of multi-electrode corona system using finite computer resource.

REFERENCES

[1] L. Dascalescu, A. Yuga, R. Morar, "Modelling of corona-electrostatic separation processes", *Material science*, vol. 16, no 1–3, pp. 273–282, 1990.

[2] D. Rafiroiu, R. Morar, P. Atten, L. Dascalescu, "Premises for the mathematical modeling of the combined corona-electrostatic field of roll-type separators", *IEEE Trans. Industry Appl.*, vol. 36, no. 5, pp. 1260–1266, 2000. [Online]. Available: http://dx.doi.org/10.1109/28.871273

[3] A. Caron, L. Dascalescu, "Numerical modeling of combined corona-electrostatic fields", *Journal of Electrostat.*, vol. 61, no. 1, pp. 43–55, 2004. [Online]. Available: http://dx.doi.org/10.1016/j.elstat.2003.12.002

[4] L. M. Dumitran, P. Atten, P. V. Notingher, L. Dascalescu, "2-D corona field computation in configurations with ionising and non-ionising electrodes", *Journal of Electrostat.*, vol. 64, no. 3–4, pp. 176–186, 2006. [Online]. Available: http://dx.doi.org/10.1016/j.elstat.2005.05.005

[5] X. Deng, K. Adamiak, "The electric corona discharge in the triode system", *IEEE Trans. Industry Appl.*, vol. 35, no. 4, pp. 767–773, 1999. [Online]. Available: http://dx.doi.org/10.1109/28.777183

[6] P. Intra, "Corona discharge in cylindrical triode charger for unipolar diffusion aerosol charging", *Journal of Electrostat.*, vol. 70, no. 1, pp. 136–143, 2012. [Online]. Available: http://dx.doi.org/10.1016/j.elstat.2011.11.007

[7] J. Miksta, S. Zebrauskas, "Analysis of the electric field in three-electrode system with corona discharge", *Material science*, vol. 16, no. 1–3, pp. 287–292, 1990.

[8] S. Zebrauskas, "Active insulation in three-electrode system", in *Proc. 13th Int. Conf. Electromagnetic Disturbances EMD 2003*, Kaunas, 2004, pp. 298–301.

[9] R. Barciauskas, S. Zebrauskas, "Numerical analysis of combined corona and electrostatic field in multi-electrode systems", in *Proc. 7th Int. Conf. Electr. and Control. Technol. (ECT 2012)*, Kaunas, 2012, pp. 235–238.

[10] S. Zebrauskas, "Corona discharge electrometer", *Defence technologies from Lithuania*, pp. 74, 2000.

[11] V. Amoruso, F. Lattarulo, "Deutch hypothesis revisited", *Journal of Electrostat.*, vol. 63, no. 6–10, pp. 717–721, 2005.

[12] L. Zhao, K. Adamiak, "EHD flow in air produced by electric corona discharge in pin-plate configuration", *Journal of Electrostat.*, vol. 63, no. 3–4, pp. 337–350, 2005. [Online]. Available: http://dx.doi.org/10.1016/j.elstat.2004.06.003

[13] R. Barciauskas, S. Zebrauskas, "Boundary conditions for combined corona and electrostatic field analysis in multi-electrode systems", in *Proc. 6th Int. Conf. Electr. and Control. Technol. (ECT 2011)*, Kaunas, 2011, pp. 264–267.

[14] J. Gudzinskas, P. Marciulionis, S. Zebrauskas, "Computation of electric wind parameters in direct current corona field", *Elektronika ir Elektrotechnika*, no. 4, pp. 3–6, 2011.

[15] R. Barciauskas, J. A. Virbalis, S. Zebrauskas, "An electrostatic approach to the numerical simulation of combined corona and electrostatic field in three-electrode system", *Elektronika ir Elektrotechnika*, no. 6, pp. 105–108, 2012. [Online]. Available: http://dx.doi.org/10.5755/j01.eee.122.6.1832

[16] R. Barciauskas, S. Zebrauskas, "Algorithms of simulation of combined corona and electrostatic fields", in *Proc. 5th Int. Conf. Electr. and Control. Technol. (ECT 2010)*, Kaunas, 2010, pp. 232–235.

[17] R. Barciauskas, S. Zebrauskas, "Computer modeling of the field in multi-electrode corona system with ionized and non-ionized areas", in *Proc. 8th Int. Conf. Electr. and Control. Technol. (ECT 2013)*, Kaunas, 2013, pp. 235–238.